

# COMBINED FORCED AND FREE-CONVECTION OVER THIN NEEDLES

JAI PRAKASH NARAIN and MAHINDER S. UBEROI

Department of Aerospace Engineering Sciences and Joint Institute for Laboratory Astrophysics,  
University of Colorado, Boulder, Colorado 80302, U.S.A.

(Received 23 September 1971 and in revised form 18 April 1972)

**Abstract**—The problem of laminar combined forced and free-convection heat transfer from a vertical thin needle in a variable external stream is considered. The similarity solutions for needles with isothermal walls and needles with uniform wall heat fluxes have been obtained. For a given value of the needle size, the flow and heat transfer behaviours are similar to those encountered with flat plates. The Nusselt number and the skin-friction coefficients increase with decreasing needle sizes for assigned values of Prandtl number, local Reynolds number, and local Grashof number.

## NOMENCLATURE

$a, b,$	needle sizes;	$r,$	radial coordinate;
$c, \hat{c},$	transformation constants;	$Re_x,$	local Reynolds number $U(x) x/\nu$ ;
$Cf_x,$	local skin-friction coefficient;	$t, t_\infty,$	local and free-stream fluid temperatures respectively;
$f,$	transformed streamfunction for isothermal wall needle;	$u, U(x),$	local axial and free-stream variable axial velocities respectively;
$g,$	transformed streamfunction for uniform wall heat flux needle;	$u_\infty,$	a constant;
$g_a,$	acceleration due to gravity;	$v,$	radial component of velocity;
$Gr_x,$	local Grashof number for isothermal needle	$x,$	axial coordinate;
		$z,$	transformed independent similarity variable for uniform wall-flux needle.
	$\frac{g_a \beta (t_w - t_\infty) x^3}{\nu^2};$		
$Gr_{x,F},$	local Grashof number for uniform wall-flux needle	Greek	
	$\frac{g_a \beta q_w x^4}{\alpha \nu^2};$	$\alpha,$	thermal conductivity;
$h,$	transformed non-dimensional temperature function for uniform wall-flux needle;	$\beta,$	coefficient of thermal expansion;
$Nu_x,$	local Nusselt number;	$\theta,$	transformed temperature function for isothermal needle;
$p,$	local pressure in the fluid;	$\Gamma,$	a parameter $Gr_{x,F}/Re_x^{5/2}$ ;
$Pr,$	Prandtl number $\nu/\kappa$ ;	$\phi,$	axisymmetric streamfunction for uniform wall-flux needle;
$q_w,$	heat flux at the wall;	$\eta,$	transformed independent similarity variable for isothermal needle;
		$\psi,$	axisymmetric streamfunction for isothermal needle;
		$\lambda,$	a parameter $Gr_x/Re_x^2$ ;

- $\nu$ , kinematic viscosity;  
 $\kappa$ , thermal diffusivity;  
 $\rho$ , ambient fluid temperature.

## Superscript

- ' , ordinary differentiation with respect to transformed independent variable.

## Subscripts

- 1, transformed variables with very large values of either  $\lambda$  or  $\Gamma$ ;  
 $w$ , wall conditions;  
 $x$ , local values at a given  $x$ .

## INTRODUCTION

THE HEAT transfer from a vertical flat plate in a variable stream and under the action of gravity has been studied numerically by Sparrow *et al.* [1] and by Brindley [2] using Meskyn's analytical methods. The problem of forced heat transfer from a thin horizontal needle in a uniform stream has been investigated by Mark [3], Tam [4] and by us [5]. Free-convection heat transfer from an isothermal vertical needle and from a uniform wall flux vertical needle under the influence of gravity has been analyzed by Cebeci and Na [6] and by us [7] respectively. These problems are closely related to similar heat transfer problems from thin vertical cylinders. Sparrow and Gregg [8], Nagendra *et al.* [9], and Fujii and Uehara [10] have considered the heat transfer from vertical cylinders under different boundary conditions. Presently we have studied the heat transfer from vertical thin needles when a variable stream is imposed on the gravity-induced convection under two distinct boundary conditions, i.e. (i) the needles with isothermal walls, and, (ii) needles with uniform wall heat fluxes. Similarity solutions have been obtained under different restrictions on the shapes of the needles and on the axial variation of free-stream velocity in the two different cases considered. The assumed boundary layer approximation is valid [5-9] for the

flow over these thin needles provided the size of the needle does not exceed the thickness of the boundary layer over it. Clearly this approximation fails near the front stagnation point of the needles and it would be valid only away from the stagnation point. The flow over such needles has considerable importance as these "needles" could be identified with very small diameter cylinders such as "wires" and the "sensors" of hot-wire anemometers.

## ANALYSIS

It has been shown [5-9] that the effect of transverse curvature cannot be neglected in such flows. Due to variable axial free-stream, an axial pressure gradient is also imposed inside the boundary layer. Retaining these effects, the equations governing the steady laminar flow in Boussinesq approximation are,

$$\frac{\partial(ru)}{\partial x} + \frac{\partial(rv)}{\partial r} = 0 \quad (1)$$

$$u \frac{\partial u}{\partial x} + v \frac{\partial u}{\partial r} = -\frac{1}{\rho} \frac{\partial p}{\partial x} + g_a \beta (t - t_\infty) + v \left( \frac{\partial^2 u}{\partial r^2} + \frac{1}{r} \frac{\partial u}{\partial r} \right) \quad (2)$$

$$u \frac{\partial t}{\partial x} + v \frac{\partial t}{\partial r} = \kappa \left( \frac{\partial^2 t}{\partial r^2} + \frac{1}{r} \frac{\partial t}{\partial r} \right) \quad (3)$$

and,

$$-\frac{1}{\rho} \frac{\partial p}{\partial x} = U(x) \frac{dU(x)}{dx} \quad (4)$$

## (i) Isothermal wall needles

Introducing the definition of axisymmetric streamfunction  $\psi$ , we transform the equations (1)-(4) with the help of the following transformations,

$$\psi = xvf(\eta), \quad t - t_\infty = (t_w - t_\infty)\theta(\eta),$$

$$U(x) = u_\infty x^{\frac{1}{2}}, \quad \eta = \left( \frac{u_\infty}{\nu} \right)^{\frac{1}{2}} \frac{r^2}{x^{\frac{1}{2}}} \quad (5)$$

The surfaces of constant  $\eta = a$  correspond to the surfaces of revolution and henceforth would be mentioned as the walls of the needles. Equation (5) transforms equations (1)–(4) to,

$$8\eta f''' + 8f'' + 4ff'' - 2f'^2 + \lambda\theta + \frac{1}{2} = 0 \quad (6)$$

$$\eta\theta'' + (1 + \frac{1}{2}Prf)\theta' = 0. \quad (7)$$

The parameter  $\lambda$  is a measure of relative importance of free-convection over forced-convection. It is given by,

$$\lambda = \frac{g_a\beta(t_w - t_\infty)}{u_\infty^2} = \frac{Gr_x}{Re_x^2}. \quad (8)$$

The proper boundary conditions could be obtained as,

$$\begin{aligned} f(a) = f'(a) = 0, \quad \theta(a) = 1 \\ f'(\infty) = \frac{1}{2}, \quad \text{and} \quad \theta(\infty) = 0. \end{aligned} \quad (9)$$

When  $\lambda$  is large, the free-convection becomes dominant over the forced-convection. In such a case, we use a transformation following [2],

$$\begin{aligned} \psi_1 = xvf_1(\eta_1), \quad t - t_\infty = (t_w - t_\infty)\theta_1(\eta_1) \\ \eta_1 = c \frac{r^2}{x^{\frac{3}{2}}}, \quad c = \left\{ \frac{g_a\beta(t_w - t_\infty)}{v^2} \right\}^{\frac{1}{2}}. \end{aligned} \quad (10)$$

The corresponding transformed similarity equations are,

$$8\eta_1 f_1''' + 8f_1'' + 4f_1 f_1'' - 2f_1'^2 + \theta_1 + \frac{1}{2\lambda} = 0 \quad (11)$$

$$\eta_1 \theta_1'' + (1 + \frac{1}{2}Prf_1)\theta_1' = 0. \quad (12)$$

The boundary conditions in these transformations are,

$$\begin{aligned} f_1(a_1) = f_1'(a_1) = 0, \quad \theta_1(a_1) = 1-0 \\ f_1'(\infty) = \frac{1}{2\sqrt{\lambda}}, \quad \text{and}, \quad \theta_1(\infty) = 0 \end{aligned} \quad (13)$$

When  $\lambda \rightarrow \infty$ , equations (11) and (12) are similar to those obtained by Cebeci and Na [6].

(ii) *Uniform wall heat flux needle*

Let  $q_w$  be the uniform heat flux through the walls of the heated needle and  $\phi$  be the axisymmetric streamfunction in the present case. We use the following similarity transformations,

$$\begin{aligned} \phi = xvg(z), \quad t - t_\infty = \frac{q_w}{\alpha} \sqrt{\left(\frac{v}{u_\infty}\right)} x^{\frac{1}{2}} h(z) \\ z = \frac{u_\infty r^2}{v x^{\frac{3}{2}}}, \quad \text{and}, \quad U(x) = u_\infty x^{\frac{1}{2}}. \end{aligned} \quad (14)$$

The similarity equations are,

$$8zg''' + 8g'' + 4gg'' - \frac{12}{5}g'^2 + \Gamma h + \frac{3}{5} = 0 \quad (15)$$

$$zh'' + h(1 + \frac{1}{2}Prg) - \frac{1}{10}Prhg' = 0. \quad (16)$$

The parameter  $\Gamma$  measures the relative strength of free-convection over the forced convective flow and is given by,

$$\Gamma = \frac{q_w g_a \beta}{\alpha u_\infty^2} \sqrt{\left(\frac{v}{u_\infty}\right)} = \frac{Gr_{x,F}}{Re_x^{\frac{3}{2}}}. \quad (17)$$

The boundary conditions at the wall  $z = b$  of the needle and far away from the needle wall ( $z \rightarrow \infty$ ) are,

$$g(b) = g'(b) = 0, \quad h(b) = -\frac{1}{2\sqrt{b}} \quad (18)$$

$$g'(\infty) = \frac{1}{2}, \quad h(\infty) = 0.$$

For free-convection dominated flows at large values of  $\Gamma$ , following [2], we used the transformations,

$$\begin{aligned} \phi_1 = xvg_1(z_1), \\ t - t_\infty = \frac{q_w}{\alpha} \sqrt{\left(\frac{v}{u_\infty}\right)} x^{\frac{1}{2}} h_1(z_1) \\ z_1 = \hat{c} \frac{r^2}{x^{\frac{3}{2}}}, \quad \hat{c} = \left[ \frac{q_w g_a \beta}{\alpha v^2} \sqrt{\left(\frac{v}{u_\infty}\right)} \right]^{\frac{1}{2}}. \end{aligned} \quad (19)$$

The similarity equations are now given by,

$$8z_1 g_1''' + 8g_1'' + 4g_1 g_1'' + h_1 - \frac{12}{5} g_1'^2 + \frac{3}{5\Gamma} = 0 \quad (20)$$

$$z_1 h_1'' + (1 + \frac{1}{2}Prg_1) h_1' - \frac{1}{10}Prh_1 g_1' = 0. \quad (21)$$

The corresponding boundary conditions at the wall  $z_1 = b_1$  and at a distance far away from the needle are,

$$g_1(b_1) = g'_1(b_1) = 0, \quad h'_1(b_1) = -\frac{1}{2\sqrt{(b_1)}} \tag{22}$$

$$g'_1(\infty) = \frac{1}{2\sqrt{(\Gamma)}}, \quad \text{and,} \quad h_1(\infty) = 0.$$

When  $\Gamma \rightarrow \infty$ , equations (20) and (21) and boundary conditions (22) are the same as those obtained by us previously [7]. Incidentally these equations are the same as those obtained by Nagendra *et al.* [9] for  $\Gamma \rightarrow \infty$ . The different form of equations (5a)–(5c) in [9] is due to the use of slightly different transformation variables.

(iii) Heat transfer and skin-friction parameters

For isothermal wall needles, we define the local Nusselt number  $Nu_x$  and the skin-friction coefficient by  $Cf_x$  by,

$$Nu_x = \frac{x(\partial t/\partial r)_{\eta=a}}{(t_w - t_\infty)} = -2\sqrt{(a)} \theta'(a) Re_x^{\frac{1}{2}} \tag{23}$$

and,

$$Cf_x = \frac{\rho\nu(\partial u/\partial r)_{\eta=a}}{\frac{1}{2}\rho U(x)^2} = 8\sqrt{(a)} f''(a) Re_x^{-\frac{1}{2}}. \tag{24}$$

For uniform wall heat flux needles, the corresponding parameters are defined as,

$$Nu_x = \frac{q_w}{\alpha(t_w - t_\infty)} = \frac{Re_x^{\frac{1}{2}}}{h(b)} \tag{25}$$

and,

$$Cf_x = 8\sqrt{(b)} g''(b) Re_x^{-\frac{1}{2}}. \tag{26}$$

The various similarity equations (6) and (7), (11) and (12), (15) and (16) and (20) and (21) were solved numerically using initial value “shooting” methods.

DISCUSSION OF RESULTS

(i) Isothermal wall needles

The non-dimensional axial velocity profiles,  $f' = u/2U(x)$  are shown in Fig. 1 for Prandtl

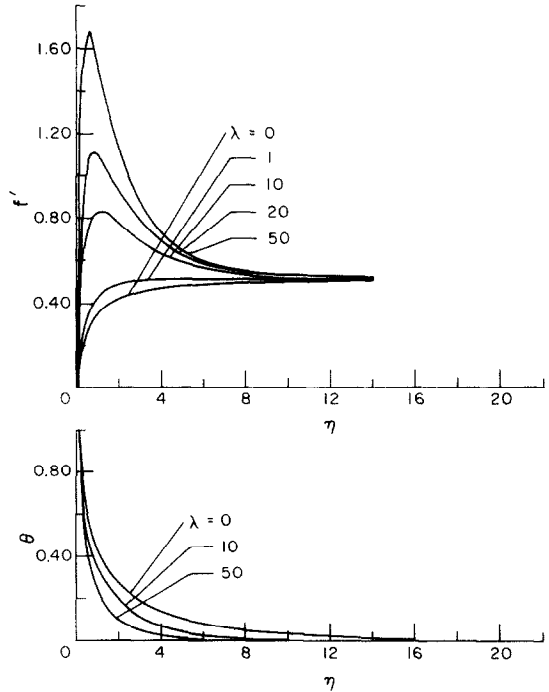


FIG. 1. Non-dimensional axial velocity,  $f'(\eta)$ , and temperature,  $\theta(\eta)$  profiles for various values of  $\lambda$ .  $Pr = 0.733$ ,  $a = 10^{-1}$ .

number,  $Pr = 0.733$ , needle size,  $a = 10^{-1}$ , and for various values of  $\lambda$ . For  $\lambda = 0$ , the gravity induced free-convection is absent and the flow is forced convection over the needle in a variable axial free-stream. This situation is different from the previously considered forced-convection over the needles in uniform stream [3–5]. The induced convection increases with increasing values of  $\lambda$  as could be noted by the rapid increase in the amount of maximum velocity. For  $\lambda \geq 20$ , the free-convection becomes dominant over the forced convection. In such a case transformed similarity equations in terms of  $f_1, \eta_1, \theta_1$ , etc. were solved numerically to obtain non-dimensional axial velocity profiles. Hence a crude limit for free-convection dominated flow regime is where,

$$Gr_x \geq 20(Re_x)^2. \tag{27}$$

The lower part of Fig. 1 shows the corresponding

variation of non-dimensional temperature function  $\theta(\eta)$ . With increasing values of  $\lambda$ , the rate of heat transfer from the needle increases, and hence the thermal boundary layer thickness decreases rapidly. For a given value of  $\lambda$  and the needle size, the broken curves in Fig. 2 show that

number. Caused by the boundary layer approximations, the above transfer behaviors are similar to that in the case of flat plates [1, 2]. Hence we conclude that for a preassigned value of the needle size, the flow and transfer behaviors are quite similar to those encountered with flat plates [3, 5-7].

The important features arising from the variation in the sizes of the needles are computed next. For a given value of  $\lambda = 1.0$  and  $Pr = 0.733$ , we have shown  $f'(\eta)$  and  $\theta(\eta)$  variations in Fig. 2 (solid curves) for two needle sizes. With progressively decreasing needle sizes, the convective increase in motion is rather slow, and hence the boundary layer thickness decreases very slowly in such a case. This slow rise in convection rates results in a slow increase in heat transfer rates. Hence the thermal layer seems to decrease very slowly in the present case.

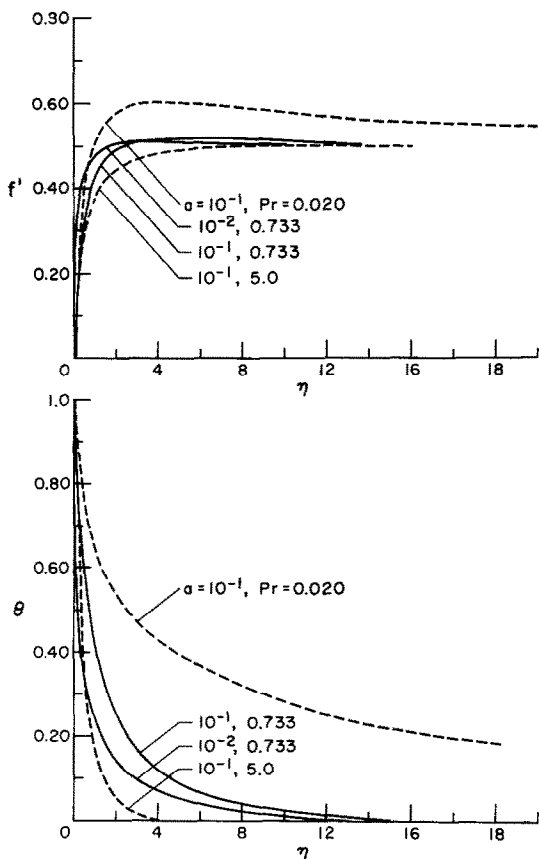


FIG. 2. Non-dimensional axial velocity,  $f'(\eta)$ , and temperature,  $\theta(\eta)$  profiles, (i) for various values of  $Pr$ ,  $a = 10^{-1}$ ,  $\lambda = 1.0$  (broken curves), and (ii) for various needle sizes  $Pr = 0.733$ ,  $\lambda = 1.0$  (solid curves).

the convective effects are suppressed whereas heat transfer rates increase rapidly with increasing value of Prandtl number. This is due to the increase in viscous diffusion over thermal diffusion with increasing values of Prandtl

Table 1. Values of  $F_1$  and  $F_2$  for  $Pr = 0.733$

Needle sizes $\lambda$	$a = 10^{-1}$		$a = 10^{-2}$	
	$F_1$	$F_2$	$F_1$	$F_2$
1.0	1.0	1.0	0.50	0.687
10.0	1.18	1.02	0.695	0.710
20.0	1.08	0.970	0.628	0.675
50.0	0.905	0.905	0.533	0.615
100.0	0.754	0.862	0.450	0.578

The Nusselt number and skin-friction coefficients could be expressed as,

$$\frac{Nu_x}{(Nu_x)_{\lambda=0}} = 1 + 0.30\lambda^{0.682}F_1(a, Pr, \lambda) \tag{28}$$

and,

$$\frac{Cf_x}{(Cf_x)_{\lambda=0}} = 1 + 0.335\lambda^{0.874} \times F_2(a, Pr, \lambda). \tag{29}$$

We have tabulated functions  $F_1(a, Pr, \lambda)$  and  $\log_{10}(1/a)F_2(a, Pr, \lambda)$  for  $Pr = 0.733$ , needle sizes,  $a = 10^{-1}$ ,  $10^{-2}$  and for various values of  $\lambda$  in Table 1. The Nusselt number was found to increase (i) with increasing values of  $\lambda$  for a given value of Prandtl number and needle size,

(ii) with increasing values of Prandtl number for given values of  $\lambda$  and needle size, and, (iii) with decreasing needle sizes at given values of  $\lambda$  and  $Pr$ . The skin-friction coefficient at a given value of local Reynolds number increases (i) with increasing value of  $\lambda$  at a given needle size and  $Pr$ , (ii) with decreasing values of Prandtl number for given values of  $\lambda$  and needle size, and (iii) with decreasing needle sizes at given values of  $\lambda$  and  $Pr$ .

(ii) *Uniform wall heat flux needles*

The uniform wall heat flux needles have

constant. Figure 3 shows the axial velocity function  $g' = u/2U(x)$  and temperature function  $h(z)$  for given  $Pr = 0.733$ , needle size  $b = 10^{-1}$ , and for various values of  $\Gamma$ . The temperature at the wall decreases with increased convection rates such that the uniform wall heat-flux condition is always maintained. The broken curves in Fig. 4 show that the influence of the Prandtl number on convection and heat transfer is similar to that in the isothermal case. The solid curves in Fig. 4 show the influence of a variation of needle sizes at a fixed value of  $Pr = 0.733$  and  $\Gamma = 1.0$ , on velocity function

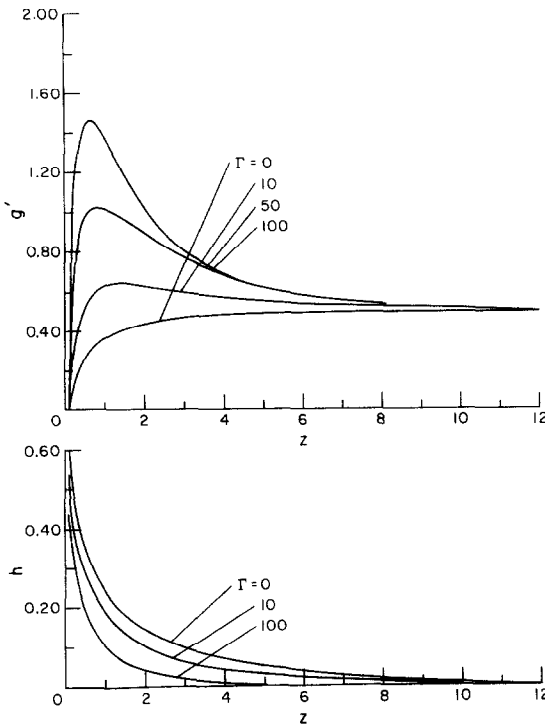


FIG. 3. Non-dimensional axial velocity,  $g'(\eta)$ , and temperature,  $h(\eta)$  profiles for various values of  $\Gamma$ ,  $Pr = 0.733$ ,  $b = 10^{-1}$ .

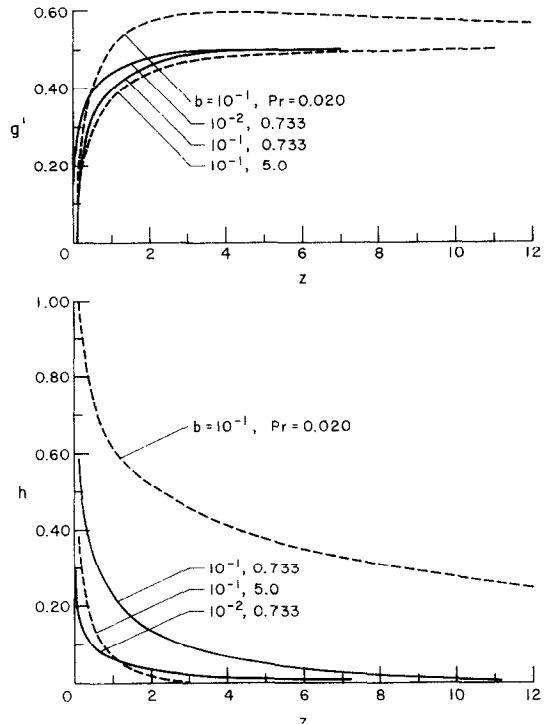


FIG. 4. Non-dimensional axial velocity,  $g'(\eta)$ , and temperature,  $h(\eta)$  profiles, (i) for various values of  $Pr$ ,  $b = 10^{-1}$ ,  $\Gamma = 1.0$  (broken curves), and (ii) for various needle sizes,  $Pr = 0.733$ ,  $\Gamma = 1.0$  (solid curves).

similar flow and transfer characteristics as those of isothermal wall temperature needles. The only major difference is in the value of wall temperature which varies according to the strength of convection to keep the flux rate

$g'(z)$  and temperature function  $h(z)$ . Except for the wall temperature changes, the basic nature of flow and heat transfer are similar to those in the case of isothermal needles.

The approximate relations for Nusselt number and skin-friction coefficient could be obtained as,

$$\frac{Nu_x}{(Nu_x)_{\Gamma=0}} = 1 + 0.02(\Gamma)^{0.682} F_3(b, Pr, \Gamma) \quad (30)$$

and,

$$\frac{Cf_x}{(Cf_x)_{\Gamma=0}} = 1 + 0.17(\Gamma)^{0.874} F_4(b, Pr, \Gamma) \quad (31)$$

where  $F_3$  and  $F_4$  are shown in Table 2. Equations (28) and (30) show that the Nusselt number ratio decreases in the case of uniform flux wall

Table 2. Values of  $F_3$  and  $F_4$  for  $Pr = 0.733$

Needle sizes $\Gamma$	$b = 10^{-1}$		$b = 10^{-2}$	
	$F_3$	$F_4$	$F_3$	$F_4$
1.0	1.0	1.0	0.17	0.353
10.0	1.145	1.065	0.364	0.412
20.0	1.10	1.005	0.390	0.406
50.0	0.940	0.892	0.382	0.391
100.0	0.795	0.825	0.348	0.370

needles. Similar observations on the Nusselt number ratio have been made by Fujii and Uehara [10]. The Nusselt number and skin-friction coefficient have similar variation with

various parameters involved as those described for isothermal wall needles.

ACKNOWLEDGEMENT

This research was supported by NSF Grant GK-27400, "A Study of Free Turbulent Vortex."

REFERENCES

1. E. M. SPARROW, R. EICHORN and J. L. GREGG, Combined forced and free-convection in a boundary layer flow, *Physics Fluids* **2**, 319 (1959).
2. J. BRINDLEY, An approximation technique for natural convection in a boundary layer, *Int. J. Heat Mass Transfer* **6**, 1035-1048 (1963).
3. R. M. MARK, Laminar boundary layers on slender bodies of revolution in axial flow, Guggenheim Aeron. Lab., Memo No. 21, Cal. Inst. of Tech. (30 July 1954).
4. K. K. TAM, On the asymptotic solutions of viscous incompressible flow past a heated paraboloid of revolution, *SIAM J. Appl. Math.* **20**, 714-721 (1971).
5. J. P. NARAIN and M. S. UBEROI, Forced heat transfer over a thin needle, *J. Heat Transfer* **94**, 240-242 (1972).
6. T. CEBECI and T. Y. NA, Laminar free-convection heat transfer from a needle, *Physics Fluids* **12**, 463-465 (1969). Erratum **13**, 536 (1970).
7. J. P. NARAIN and M. S. UBEROI, Free-convection heat transfer from a thin vertical needle, *Physics Fluids* **15**, 928-929 (1972).
8. E. M. SPARROW and J. L. GREGG, Laminar-free-convection heat transfer from the outer surface of a vertical circular cylinder, *Trans. Am. Soc. Mech. Engrs* **78**, 1823-1829 (1956).
9. H. R. NAGENDRA, M. A. TIRUNARAYANAN and A. RAMACHANDRAN, Laminar free convection from vertical cylinders with uniform heat flux, *J. Heat Transfer* **92**, 191-194 (1970).
10. T. FUJII and H. UEHARA, Laminar natural-convection heat transfer from the outer surface of a vertical cylinder, *Int. J. Heat Mass Transfer* **13**, 607-615 (1970).

CONVECTION MIXTE AUTOUR D'AIGUILLES FINES

**Résumé**—On considère le problème du transfert thermique par convection laminaire mixte sur une fine aiguille verticale dans un courant externe variable. On a trouvé les solutions de similarité pour des aiguilles avec paroi isotherme et pour des aiguilles avec flux thermique pariétal uniforme. Pour une taille d'aiguille donnée les comportements de l'écoulement et du transfert thermique sont semblables à ceux considérés pour des plaques planes. Le nombre de Nusselt et les coefficients de frottement pariétal croissent inversement aux tailles des aiguilles pour des valeurs données du nombre de Prandtl, du nombre local de Reynolds et du nombre local de Grashof.

**Zusammenfassung**—Das Problem laminarer, kombinierter erzwungener und freier konvektiver Wärmeübertragung von einer dünnen Nadel bei veränderlicher Anströmung wird behandelt. Die ähnlichen Lösungen für Nadeln mit isothermen Wänden und Nadeln mit einheitlichen Wandwärmeströmen wurden erhalten. Für einen gegebenen Wert der Nadelform sind Strömungs- und Wärmeübertragungsverhalten ähnlich denen, die man bei flachen Platten erhält. Die Nusselt-Zahl und der Oberflächenreibungskoeffizient erhöhen sich mit abfallender Nadelform für bestimmte Werte von Prandtl-Zahl, lokaler Reynolds-Zahl und lokaler Grashof-Zahl.

ТЕПЛООБМЕН ПРИ ВЫНУЖДЕННОЙ И СВОБОДНОЙ КОНВЕКЦИИ У  
ТОНКИХ СТЕРЖНЕЙ

**Аннотация**—Рассматривается задача о совместном теплообмене между вертикальным тонким стержнем и переменной внешней средой при капиллярной вынужденной и свободной конвекции. Получены автомодельные решения для стержней с изотермическими границами и стержней с однородными тепловыми потоками на стенках. Для стержня данного размера режимы течения и теплообмена сходны с режимами для плоских пластин. При заданных значениях числа Прандтля, локальных чисел Рейнольдса и Грасгофа число Нуссельта и коэффициенты поверхностного трения увеличиваются с уменьшением размеров стержня.